ISSN 2278-3091

Volume 9, No.1.5, 2020

International Journal of Advanced Trends in Computer Science and Engineering

Available Online at http://www.warse.org/IJATCSE/static/pdf/file/ijatcse0591.52020.pdf

https://doi.org/10.30534/ijatcse/2020/0591.52020

Control of WECS Involving DFIG Using Backstepping Technique Based On High Gain Observer

Youssef Baala[1], Seddik Bri[1]

[1] MIM, High School of Technology, Moulay Ismail University, Meknes, Morocco

ysfbaala@gmail.com, briseddik@gmail.com

ABSTRACT

This article deals with the problem of controlling a wind energy conversion system (WECS) based on the doubly fed induction generator (DFIG). The purposed control is to maximize the extraction of wind energy while letting the wind turbine rotor operate in variable speed mode. This work highlights the achievement of the above energy objective without using any wind speed sensor. The control strategy uses a non-linear regulator designed by the backstepping technique and based on the use of a high gain observer; fitted with a sensor less online reference speed optimizer designed using the power characteristic of the turbine to ensure maximum power point tracking (MPPT). The proposed controller achieves the desired performance and this is confirmed by several simulations.

Key words: DFIG, High gain observer, Backstepping, MPPT, Sensor less, Wind energy conversion

1. INTRODUCTION

Currently large wind turbines operate at variable speed. The most suitable generator is the doubly-fed asynchronous motor called DFIG. This generator is characterized by only 20% to 30% of the power must pass by frequency conversion from 100% for the variable speed synchronous generator [1]. This gives a reduction of the cost of the converters involved. The design of a nonlinear output backstepping control with suitable nonlinear observers allow to obtain interesting results. Observers were designed in return output control by Lipschitz.The quadratic function of Lyapunov [3] can be used to design this observer. This observer is based on the high gain.

The design of the observer and the DFIG control presented in this work offers a sensor less controller avoiding the measurement of mechanical variables and flux and supporting a wide variation of all system state variables guarantee one flow control to ensure linear behavior of the DFIG magnetic circuit and a DC bus control voltage to protect the inverter in question and rectifier in addition the power factor correction for injecting clean energy as a goal of MPPT [4]. The results are validated by simulation in the MATLAB / SIMULINK environment.

2. SYSTEM MODELING

2.1 Control structure

The configuration of DFIG wind turbine selected for this work is that of the following structure (Figure 1), which allows full control using rotor signals. This structure uses two static converters, one on the rotor CCR rectifier side the other side of the inverter GCR network based on insulated gate bipolar transistors (IGBT) and controlled by pulse width modulation (PWM).Control MPPT is used to calculate the machine rotation online speed reference ωref, to ensure extraction of the maximum power of the wind turbine[5].

A high gain observer delivers an estimate at the exit of this block value of mechanical torque TG and rotation speed ω. We use electrical quantities measurable to avoid mechanical quantities not measurable, in our study the speed of the rotor, the mechanics torque T_G and wind speed v.

The system must ensure maximum power extraction of the turbine and the electrical energy supplied to the network while ensuring the requirements imposed by the electrical network. The control consists of the following blocks [6]:

- A rotor speed controller ω to follow the reference speed ω_{ref} emitted by the MPPT block.
- A reactive power regulator Q_N supplied to network equal to a Q_{Nref}=0 reactive power reference.
- A stator flow controller ϕs ensuring its maintenance at its nominal value ϕ_{sN}.
- A voltage regulator V_{dc} across capacitor C which must follow a reference V_{dcref} value to protect the power switches.

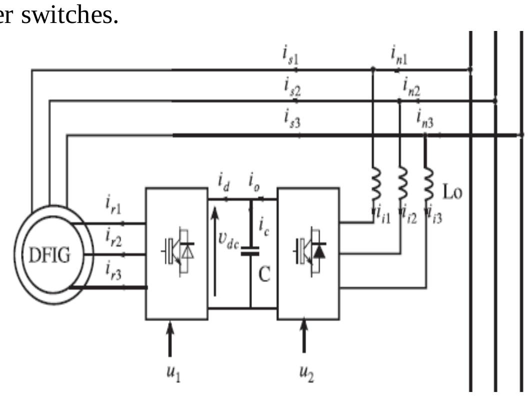

Figure 1: Connection of converters with the DFIG machine

2.2 The DFIG modeling

The DFIG model of stator flux and rotor variables used for this control are detailed in equations [1,2]. Since the stator is directly connected to the electrical network, we conclude:

$v_{sd} = E_{Nd}$ and $v_{sq} = E_{Nq}$. The equations connecting the PWM control rectifier with the electrical quantities conveyed are written: $id = u_1^T.i_r$ and $v_r = u_1.v_{dc}$, with $u1 = [u_{1d}, u_{1q}]$ T, then we can write the model of systems involving the rectifier PWM control (u_{1d}, u_{1q}) [7]:

$$\dot{x}_1 = p\,\frac{M_{sr}}{JL_s}\,(x_3x_4 - x_2x_5) - \frac{T_G}{J} - \frac{f_v}{J}x_1 \quad (1)$$

$$\dot{x}_2 = -\frac{1}{\tau_s}x_2 + \omega_s x_3 + \frac{M_{sr}}{\tau_s}x_4 + E_{Nd} \quad (2)$$

$$\dot{x}_3 = -\frac{1}{\tau_s}x_3 - \omega_s x_2 + \frac{M_{sr}}{\tau_s}x_5 + E_{Nq} \quad (3)$$

$$\dot{x}_4 = -\gamma_1 x_4 + (\omega_s - px_1)x_5 + \frac{\gamma_2}{\tau_s}x_2 - p\gamma_2 x_1x_3 - \gamma_2 E_{Nd} + \gamma_3 u_{1d}v_{dc} \quad (4)$$

$$\dot{x}_5 = -\gamma_1 x_5 + (\omega_s - px_1)x_4 + \frac{\gamma_2}{\tau_s}x_3 + p\gamma_2 x_1x_2 - \gamma_2 E_{Nq} + \gamma_3 u_{1d}v_{dc} \quad (5)$$

With $\gamma 1$, $\gamma 2$, $\gamma 3$, σ and τs :

$$\gamma_1 = \frac{R_rL_s^{\,2} + R_sM_{sr}^{\,2}}{\sigma L_rL_s^{\,2}} \quad , \quad \gamma_2 = \frac{M_{sr}}{\sigma L_sL_r}$$

$$\gamma_3 = \frac{1}{\sigma L_r} \quad ,\sigma = 1 - \frac{M_{sr}^{\,2}}{L_sL_r} \quad ,\tau_s = \frac{L_s}{R_s}$$

The differential equation governing the voltages v_{dc} and currents i_{id} and i_{iq}:

$$\frac{d(v_{dc}^2)}{dt} = -\frac{2}{C}\left(E_{Nd}i_{id} + E_{Nq}i_{iq}\right) - \frac{2}{C}v_{dc}i_d \quad (6)$$

$$\frac{di_{id}}{dt} = \frac{E_{Nd}}{L_0} + \omega_s i_{iq} + \frac{v_{dc}}{L_0}u_{2d} \quad (7)$$

$$\frac{di_{iq}}{dt} = \frac{E_{Nq}}{L_0} - \omega_s i_{id} + \frac{v_{dc}}{L_0}u_{2q} \quad (8)$$

T_{em} as measurable state variable,and knowing that :

$$T_{em} = p.M_{sr}i^T.T_0.i \quad (9)$$

With: $T_0 = \begin{bmatrix} O_2 & J_2 \\ O_2 & O_2 \end{bmatrix}$ $O_2 = \begin{bmatrix} 0 & 0 \\ 0 & 0 \end{bmatrix}$ $J_2 = \begin{bmatrix} 0 & -1 \\ 1 & 0 \end{bmatrix}$

$$\dot{T}_{em} = S_1(i,\nu) - S_2(i)\omega \quad (10)$$

With $S_1(i,\nu) = 2pM_{sr}i^TT_0\,(\gamma M_1\nu + M_{23}i$

$S_2(i) = 2p^2\gamma M_{sr}i^TT_0\,M_4 i$

We deduce the equations of system [8]:

$$\begin{cases} \dot{T}_{em} = S_1(i,\nu) - S_2(i)\omega \\ \dot{\omega} = \frac{1}{J}(T_{em} - T_G - f_v\omega) \\ \dot{T}_{G} = \varepsilon(t) \end{cases} \quad (11)$$

2.3 High gain observer

If we use this transformation, we can write the system ender normalized form [8]:

$$\xi = \phi(x) = \begin{bmatrix} x_{01} \\ -S_2(i)x_{02} \\ \frac{S_2(i)}{J}x_{03} \end{bmatrix}$$

$$\begin{cases} \dot{\xi} = A\xi + \psi(\xi) + \epsilon(t) \\ y_1 = x_1 \end{cases} \quad (12)$$

The Jacobian is given by[8]:

$$\Lambda = \frac{d\xi}{dt} = \begin{bmatrix} 1 & 0 & 0 \\ 0 & -S_2(i) & 0 \\ 0 & 0 & \frac{S_2}{J} \end{bmatrix} \quad (13)$$

Consider the system (12), then the high gain observer can be used to estimate online system state variables:

$$\dot{\hat{\xi}} = A\hat{\xi} + \psi(\hat{\xi}) + \theta\Delta_\theta^{\;-1}S^{-1}C^T(\hat{\xi} - \xi) \quad (14)$$

Where θ is the observer gain, $\Delta\theta$ = diag[1, $1/\theta$, $1/\theta^2$], and S is a symmetric positive definite matrix, it is the unique solution of the following Lyapunov equation:

$S + A^TS + SA - C^TC = 0$.

This observer is globally exponentially stable.

The observation Errol is written: $\breve{x} = \hat{x} - x$

The convergence of the following Lyapunov function [9]:

$V = \bar{x}^T\ S\ \bar{x}$ .We can assume φ is considered Lipchitzian.

For $\theta > \theta_0 > 0$, we can establish the following inequality:

$\breve{T}_a = \widehat{T}_a - T_a$

In terms of trajectory tracking, we make the following error:

$$\mathbf{e_T = T_{opt} - T_a} \quad (15)$$

Where Ta is deduced from the observer. We are getting:

$$\mathbf{\dot{e}_T = 2\ kopt\ \omega\ (Ta - Kt\ \omega - Tg) - \dot{T}a} \quad (16)$$

The super twisting algorithm allows writing:[10]

The super twisting algorithm allows writing:[10]

$$\begin{cases} Tg = y + B1.\,e_T^{\frac{1}{2}}\,sgn(e_T) \\ \dot{y} = B2\,sgn(e_T) \end{cases} \quad (17)$$

So we can say that there is a finite time tc, T_a converges to T_{opt} such that: $T_a = T_{opt}$ when t >tc

2.4 Design of backstepping control

The objective is to seek a reference speed ωopt, to reach the optimal working speed conditions of the wind turbine and thus capture the maximum energy the wind. Wind energy captured by the turbine is a function of area A, air density ρ and the wind speed v. The transmitted power P of wind energy is written as a function of power coefficient Cp [1]:

$$P_{wind} = \frac{1}{2}.\rho.AV_{wind}^{\;\;3} \quad (18)$$

Fig.2 shows the optimum mechanical power, recovered by the turbine, as a function of the angular speed of the rotor.

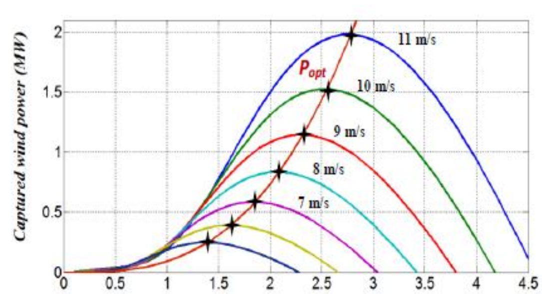

Figure 2: Variation of captured wind power (Pitch angle β=0°)

The optimum mechanical power Popt is given by [8]:

$$\begin{cases} Ta = K\omega \\ Kopt = \frac{1}{2}\,\rho.\pi.R^5\,\frac{Cpmax}{\lambda opt^3} \end{cases} \quad (19)$$

Where λopt is the specific speed that allows us to maximize the power captured. The goal of the following strategy is that Ta converges to Topt while the standard law imposes that T_G = Topt. This simplification amounts to neglecting the effect of mechanical transmission induces a loss of efficiency.

The vertices of these curves give the maximum of P_{opt} power and therefore represent the optimal points [11].

$$F(P) = h_n P^n + h_{n-1}P^{n-1} + \cdots + h_1 P + h_0 \quad (20)$$

Each of these points is characterized by the optimum speed *ω*opt. Figure 2 easily shows that for any wind speed value vi, there is a unique couple (*ω*i, Pi) which involves the greatest extractable power. All of all these optimal couples (*ω*i, Pi) are represented in the figure curve. These couples were interpolated to obtain a polynomial function ω_{opt} = F (P_{opt}). The optimal point calculation algorithm is as follows [12]:

-At the beginning we assume that at t = 0 the wind speed is v0 and the rotor speed is *ω*0.

-We can calculate online from the curve to which transmitted wind power P0 corresponds this couple (v0, *ω*0).

- Given the value of P0, the speed reference optimizer gives new rotor speed reference value *ω*1 = F (P0).

a well-defined cruise control turns the rotor of the machine to the new speed reference, *ω* = *ω*1. - according to the curve wind turbine provides new extractable power value equal to P1. And the speed reference optimizer provides to the cruise control a new speed reference *ω*2.

-This block will be repeated until completion from the Optimal point(Popt,*ω*opt).

If one uses the following changes of variables:

$x_6 = v^2_{dc}$, $x_7 = i_{id}$ and $x_8 = i_{iq}$, and knowing that the rotation speed x1 and the mechanical torque T_G are delivered by the high gain observer mentioned below.

We can put the system under the following form [13-14]:

$$\begin{cases} \dot{\hat{x}}_1 = \frac{\hat{T}_{em}}{J} - \frac{f_v\hat{x}_1}{J} - \frac{\hat{T}_G}{J} + 3\theta^2 S_2^{-1}(i)\left(\hat{T}_{em} - p\frac{M_{sr}}{L_s}(x_3x_4 - x_2x_5)\right) \\ \dot{x}_2 = -\frac{1}{\tau_s}x_2 + \omega_s x_3 + \frac{M_{sr}}{\tau_s}x_4 + E_{Nd} \\ \dot{x}_3 = -\frac{1}{\tau_s}x_3 - \omega_s x_2 + \frac{M_{sr}}{\tau_s}x_5 + E_{Nq} \\ \dot{x}_4 = -\gamma_1 x_4 + (\omega_s - p\hat{x}_1)x_5 + \frac{\gamma_2}{\tau_s}x_2 - p\gamma_2\hat{x}_1x_3 - \gamma_2 E_{Nd} + \gamma_3 u_{1d}V_{dc} \\ \dot{x}_5 = -\gamma_1 x_5 - (\omega_s - p\hat{x}_1)x_4 + \frac{\gamma_2}{\tau_s}x_3 + p\gamma_2\hat{x}_1x_2 - \gamma_2 E_{Nq} + \gamma_3 u_{1q}V_{dc} \\ \dot{x}_6 = -\frac{2}{C}(E_{Nd}x_7 + E_{Nq}x_8) - \frac{2}{C}v_{dc}i_d \\ \dot{x}_7 = \frac{E_{Nd}}{L_0} + \omega_s x_8 + \frac{v_{dc}}{L_0}u_{2d} \\ \dot{x}_8 = \frac{E_{Nq}}{L_0} - \omega_s x_7 + \frac{v_{dc}}{L_0}u_{2q} \end{cases} \quad (21)$$

Te control of the rotation speed *ω* = x_1 and the flux norm $\phi = x_2^2 + x_3^2$ should be noted that if the machine is driven at the reference rotation speed *ω*ref (delivered by the MPPT-bloc), therefore it ensures the extraction of the maximum power from the wind turbine.

The flux reference is set to its nominal value.We will design the controller in two steps using the backstepping technique and introduce two errors e1 and e2 :

$$\begin{cases} e_1 = \omega_{ref} - \hat{x}_1 \\ e_2 = \phi^2{}_{ref} - (x_2{}^2 + x_3{}^2) \end{cases}$$

(22)

The errors dynamics e1 and e2 can be represented by :

$$\begin{cases} \dot{e}_1 = \dot{\omega}_{ref} - \frac{\hat{T}_{em}}{J} + \frac{f_v\hat{x}_1}{J} + \frac{\hat{T}_G}{J} - 3\theta^2 S_2{}^{-1}(i) * \\ \quad \left(\hat{T}_{em} - p\frac{M_{sr}}{L_s}(x_3x_4 - x_2x_5)\right) \\ \dot{e}_2 = 2\phi_{ref}\dot{\phi}_{ref} - 2\left(\frac{1}{\tau_s}(M_{sr}(x_2x_4 + x_3x_5) - \right. \\ \quad \left.(x_2{}^2 + x_3{}^2))\right) - 2(x_2E_{Nd} + x_3E_{Nq}) \end{cases} \quad (23)$$

let's consider the following Lyapunov function:

$V_1 = 0.5.e_1^2$ and $\dot{V}_1 = -c_1 e_1{}^2$

where c1 is a positive control parameter.

This proves the global and asymptotic stability of the system.The second stage of conception consists in choosing the real control signals u_{1d} and u_{1q}, so that any errors (e1, e2, e3, e4) converge to zero. To this end, we should explain how these errors depend on the real control signals (u_{1d}, u_{1q}).

$$\dot{e}_3 = F_3(x,\hat{x}) - 3p\frac{M_{sr}}{L_s}\theta^2 S_2{}^{-1}(i)\gamma_3 V_{dc}(x_3u_{1d} - x_2u_{1q})$$

$$\dot{e}_4 = G_4(x) - 2\frac{M_{sr}}{\tau_s}\gamma_3 V_{dc}(x_2u_{1d} + x_3u_{1q})$$

(24)

To analyze the system error (45-48), lets consider the augmented Lyapunov function [14]:

$$V_2 = \frac{1}{2}(e_1{}^2 + e_2{}^2 + e_3{}^2 + e_4{}^2) \quad (25)$$

Its derivative in time along the trajectory of the state vector (e1, e2, e3, e4) is:

$$\dot{V}_2 = e_1\dot{e}_1 + e_2\dot{e}_2 + e_3\dot{e}_3 + e_4\dot{e}_4 \quad (26)$$

We can choose the controls inputs u_{1d} and u_{1q} to cancel the term between parentheses multiplying e_3 and e_4 in the Lyapunov equation derivative .Both controls exist if the matrix $X = \begin{pmatrix} x3 & -x2 \\ x2 & x3 \end{pmatrix}$ is non-singular.

The determinant of this matrix is equal to $x_2^2 + x_3^2$ which is the stator flux in the machine. The flux cannot be zero, because the stator is all time connected to the grid. Then the controls u_{1d} and u_{1q} can be written as:

$$\begin{pmatrix} u_{1d} \\ u_{1q} \end{pmatrix} = X^{-1}\begin{pmatrix} c_3e_3 + F_3(x,\hat{x})\frac{L_S S_2(i)}{3pM_{sr}\theta^2\gamma_3 V_{dc}} \\ c_4e_4 + G_4(x)\frac{\tau_s}{2M_{sr}\gamma_3 V_{dc}} \end{pmatrix} \quad (27)$$

The control signals in the Lyapunov function derivative which proves the asymptotic stability of the considered speed control.

The system composed by the DFIG, described by the model, and nonlinear control laws has the following properties [15]:

- The closed loop system represented in the coordinates (e1, e2, e3, e4), by the following equations:

$$\begin{cases} \dot{e}_1 = -c_1e_1 - e_3 \\ \dot{e}_2 = -c_2e_2 + e_4 \\ \dot{e}_3 = -c_3e_3 \\ \dot{e}_4 = -c_4e_4 \end{cases} \quad (28)$$

Assume that the control parameters c1 and c2 are large enough in the sense that C1 > 12 and C2 > 12 . Then,all errors e1, e2, e3, e4 are asymptotically, regardless of the initial conditions.The system is globally asymptotically stable,relating to the Lyapunov equation V2. Consequently, the errors (e1, e2, e3, e4) vanish exponentially fast, whatever the initial conditions.

2.5 Controller of the vdc voltage and PFC

The injected energy, should not pollute the network. So,the currents in1, in2 and in3 have to be sinusoidal and in phase with the electrical grid voltages e_{N1}, e_{N2} and e_{N3} [16].
For this, the reactive power must be equal to reactive power reference Qn* and the voltage across the capacitor vdc must be equal to a voltage reference vdcref.
let's introduce errors e5 on the voltage control vdc and e6 on the reactive power control.

$e_5 = v^2_{dcref} - x_6$ and $e6 = Q_N^* - Q_N$

$$Q_N = E_{Nd}\, i_{Nq} - E_{Nq}\, i_{Nd}, \tag{29}$$

The dynamics errors e5 and e6 can be represented by:

$$\dot{e}_5 = 2v_{dref}\dot{v}_{dref} + \frac{2}{C}\left(E_{Nd}x_7 + E_{Nq}x_8\right) + \frac{2}{C}v_{dc}i_d \tag{30}$$

$$e_6 = \dot{Q}_N^* - E_N^T J_2\left(\frac{\dot{x}_{23}}{L_s} - \frac{M_{sr}}{L_s}\dot{x}_{45}\right) - E_{Nd}\dot{x}_8 + E_{Nq}\dot{x}_8 \tag{31}$$

With : $E_N = \begin{pmatrix} E_{Nd} \\ E_{Nq} \end{pmatrix}$, $x_{23} = \begin{pmatrix} x_2 \\ x_3 \end{pmatrix}$, $x_{45} = \begin{pmatrix} x_4 \\ x_5 \end{pmatrix}$, $J_2 = \begin{pmatrix} 0 & -1 \\ 1 & 0 \end{pmatrix}$

3.RESULTS AND ANALYSIS

The performances of the controller is been validated by means of simulation in MATLAB/Simulink environment. The table summarizes the parameters of the controlled system.

Turbine Power P_N= 1.5 MW

Turbine Inertia J=4.4532×105 kg m

GADA:
Number of pole pairs: p=2
Stator Résistance Rs=0.005 Ω
Stator Inductance Ls= 0.40744 mH
Rotor Résistance Rr=0.0089 Ω
Rotor Inductance Lr=0.29921 mH
Mutuel inductance M=0.0016 mH
Command:
B1 = 1.5, B2 = 50, B3= 200 .
θ = 30 ,C1 = 5000, C2= 100000, Kopt = 161240.

This simulation, Fig.3 presents, a step of wind speed varying between 6.5 m/s and 13 m/s applied to the inlet of the turbine.

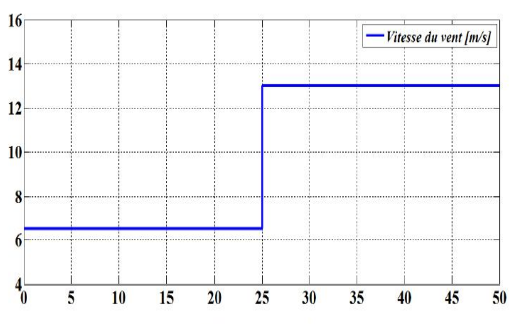

Figure 3: Step variation of wind speed

The fig.4 illustrates a perfect continuation of the electromagnetic torque at its reference delivered by the observer block in reduce time 2.5 s. We note the convergence of the electromagnetic torque Tem towards the optional reference torque Topt a variation from 2500 Nm to 12500Nm corresponding to the characteristics of a 1.5 MW wind turbine.

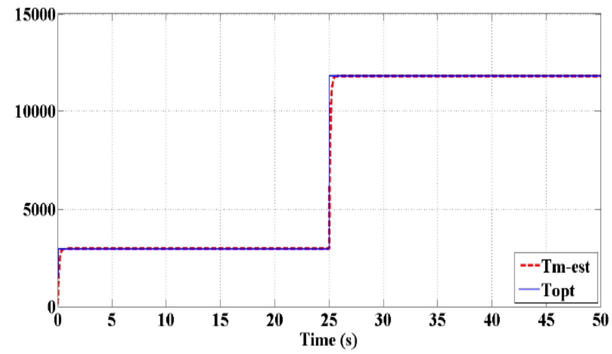

Figure 4: Variation of electromagnetic torque for step wind speed

We note in Fig.5 the variation of the power Ps produced by the DFIG to the network from 1Mw to 1.2 Mw according to the maximum point of the wind while garanteissant a unit cosφ by regulation which guarantees the cancellation of the reactive power Qs.

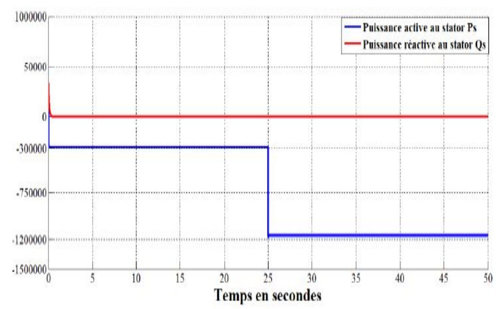

Figure 5: Powers variation for step wind speed

In this simulation Fig.6, a random of wind speed is applied to the inlet of the turbine varying between 6.5 m/s to 12.5 m/s.

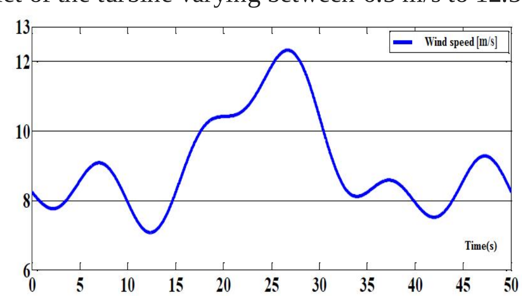

Figure 6: Pseudo-random variation of wind speed

We show in Fig.7 a perfect continuation of the electromagnetic torque at its reference delivered by the observer block varying between 800Nm and 1200 Nm. We note the convergence of the electromagnetic torque Tem towards the optional reference torque T_{opt} despite a tolerable overshoot.

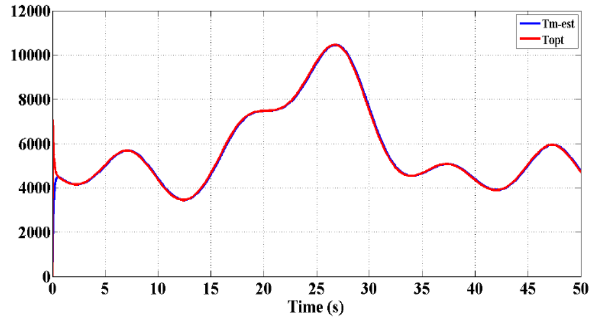

Figure 7: Variation of electromagnetic torque for random wind speed

Fig.8 demonstrated the various active power P supplied to the network goes from a production up to nominal production 1.5 Mw. The stator reactive power Q is kept zero to guarantee a unit power factor cosφ= 1.

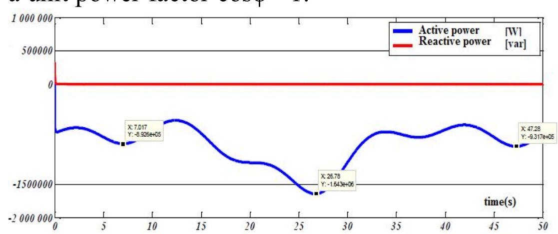

Figure 8: Powers variation for random wind speed

Fig.9 indicates that despite the pseudo-random variation of the wind, we obtain a sinusoidal three-phase current output with minimal distortion With a THD harmonic distortion rate of 0.05.

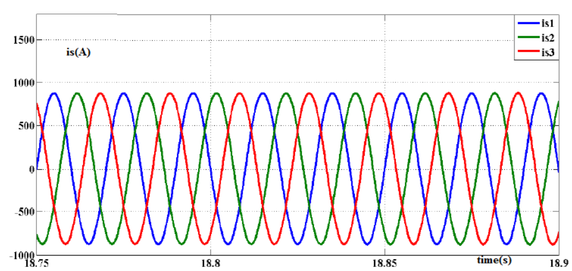

Figure 9: Stator current

The results of the command show that the production of electrical energy by the DFIG on the network is done in optimal conditions minimizing the losses so a production at maximum efficiency quantified around 67%.

3. CONCLUSION

In this paper, we studied a backstepping control without speed and torque sensors of the wind turbine system based on doubly fed induction generator DFIG connected to the grid with a PWM converter AC/DC/AC. The reference of the machine rotational speed is issued from the MPPT block based on the electric power injected into the grid measurement. It has been demonstrated the control laws, and the stability by Lyapunov method. A simulation of the control law in the MATLAB/SIMULINK environment, demonstrate satisfactory dynamic performances of this control. The sensor-less control shows a good performance at high and low speed of the DFIG without overshoot. The currents and voltages on the rotor and stator are sinusoidal, generally, very easy to measure. The estimated speed and torque converge immediately to their respective optimal values.

REFERENCES

1. Youssef Baala,Seddik Bri **"Torque Estimator using MPPT Method for wind Turbines "**International Journal of Electrical and Computer Engineering (IJECE) Vol.10, No.2 , April 2020, pp. 1208-1219
2. Abdelwahed Touati, and all **Improved Strategy of an MPPT Based on the Torque Estimator for Variable Speed Turbines** IREMOS Vol 8 N 6 2015
3. Rachid Lajouad and All **Output feedback control of wind energy conversion system involving a doubly fed induction generator**Asian J Control. 2019; pp1–11.
4. H. Becheri , I. K. Bousarhanne , A. Harrouz , H. Glaoui , T. Belbekri, "**Maximum Power Point Tracking of Wind Turbine Conversion Chain Variable Speed Based on DFIG,**" International Journal of Power Electronics and Drive System (IJPEDS), vol. 9, no. 2, pp. 527-535, Jun. 2018.
5. Dwiana Hendrawati1, Adi Soeprijanto, Mochamad Ashari, "**High Performance Maximum Power Point Tracking on Wind Energy Conversion System**," International Journal of Power Electronics and Drive System (IJPEDS), vol. 8, no. 3, pp. 1359-1367, Sep. 2017.
6. Abdellah Boualouch , Tamou Nasser, Ahmed Essadki , Ali Boukhriss **DFIG power reserve control based on ADRC during grid frequency fault** International Journal of Advanced Trends in Computer Science and Engineering IJATCSE,2019 Vol 8, pp 426-431
7. Deshpande, Anjalic. **Active and Reactive Voltage Control for DFIG Interface** International Journal of Advanced Trends in Computer Science and Engineering IJATCSE,2019 Vol 8. pp 3375-3380.
8. O. Naifar et al., **Global practical mittag leffler stabilization by output feedback for a class of nonlinear fractional-order** systems,Asian J. Control 20 (2018), 599–607.
9. A.-L. Olimpo et al., **Wind Energy Generation Modelling and Control,** JohnWiley & Sons, Chichester, 2009.
10. C. Tutivén et al., **Hysteresis-based design of dynamic reference trajectories to avoid saturation in controlled wind turbines,** Asian J.Control 19 (2017), pp 438–449.
11. F.-J. Lin, S.-G. Chen, and I.-F. Sun, Adaptive **backstepping control of six-phase pmsm using functional link radial basis function network uncertainty observer**, Asian J. Control 19 (2017), pp 2255–2269.
12. T. Nguyen et al., **Real-time sliding mode observer scheme for shear force estimation in a transverse dynamic force microscope**, Asian J. Control 20 (2016), pp 1317–1328.
13. S. Routray, R. Patnaik, and P. Dash, **Adaptive non-linear control of upfc for stability enhancement in a multimachine power system operatingwith a dfig based wind farm,**Asian J. Control 19 (2017),1575–1594.
14. Boukhezzar B. et al. **Multivariable control strategy for variable speed variable pitch wind turbine. Renewable Energy,** vol. 32, pp. 1273-1287, 2007.
15. Touati Abd el Wahed ALL Design of an Mppt based on the torque estimator for variable speed turbines ICEIT 2015

    N. Amuthan, et al., " **Voltage sag ride through using Improved Adaptive Internal Model Controller for doubly fed induction generator wind farms**", Computers and Electrical Engineering, 2013.